Biochimica et Biophysica Acta, 979 (1989) 321–330
Elsevier

BBA 74341

The different influences of ether and ester phospholipids on the conformation of gramicidin A. A molecular modelling study

Gijsbert H.W.M. Meulendijks, Trudi Sonderkamp, Joost E. Dubois, Roman J. Nielen, John A. Kremers and Henk M. Buck

Department of Organic Chemistry, Eindhoven University of Technology, Eindhoven (The Netherlands)

(Received 24 October 1988)

Key words: Molecular modeling; Gramicidin A; Phosphatidylcholine; AMBER

With AMBER (assisted model building with energy refinement) molecular modelling techniques, the interactions between lipids which differ in the type of chain linkage (e.g., ether or ester) and gramicidin were approximated. It was found, theoretically, that replacement of the ester function in dipalmitoylphosphatidylcholine (DPPC) by an ether moiety induces a shift in the rotameric distribution of the Trp-15 side-chain in gramicidin A. Concomitantly, the channel entrance is contracted by approx. 0.4 Å. The perturbation can be related to the strong hydrogen-bond formed between the lipid carbonyl group and the indole proton of the Trp-15 residue of gramicidin. In the ether lipid-gramicidin assembly a weaker H-bond is formed between Trp-15 and the phosphate moiety. To obtain a first indication of the influence of the strength of this H-bond on gramicidin A, a preliminary experimental study was set up. The transport properties of gramicidin A were studied using efflux measurements through vesicle walls containing ether and ester lipids, respectively. A change in the permeability of gramicidin A was found when ether lipids were added to a bilayer composed of the ester lipid dioleoylphosphatidylcholine (DOPC).

Introduction

Numerous studies have been conducted on protein–lipid interactions, but only few are concerned with the question of whether lipids are capable of modifying the conformation of membrane proteins. Phospholipids, in particular, are very well suited to transfer information from the easily accessible headgroups to the hydrophobic part of the membrane [1]. Recently, a mechanism was outlined by which the formation of a five-coordinated TBP phosphorus atom in the phospholipid headgroup can be transmitted via intramolecular electrostatic repulsions in the glyceryl backbone to the hydrocarbon chains [2,3].

Because of the enhanced electron density on the axially located *sn*-3 oxygen atom, an increased electrostatic repulsion between the *sn*-2 and the *sn*-3 oxygen atoms occurs. As a result of this increased repulsion, the conformational equilibrium in the glyceryl backbone changes [3]. This altered conformational equilibrium can induce a more tight chain packing in the solid phase (Meulendijks, G.H.W.M., De Haan, J.W., Van Genderen, M.H.P. and Buck, H.M., personal communication). It can be imagined that by adopting a different phospholipid chain packing, the structure of embedded proteins may very well be modified. For instance, it has been argued, based on theoretical investigations, that the channel-forming polypeptide gramicidin A can be influenced by the lipid environment via conformational changes in the peptide residues, resulting in different conductivities through the channel [4].

Gramicidin A is an extensively investigated peptide, but very little is known about its molecular interactions with lipids. The peptide consists of 15 alternating D- and L-amino acids [5]:

HCO-L-Val-Gly-L-Ala-D-Leu-L-Ala-D-Val-L-Val-D-Val-L-Trp-D-Leu-L-Trp-D-Leu-L-Trp-D-Leu-L-Trp-NH(CH_2)$_2$OH

(1 5 10 15)

Abbreviations: DMPC, dimyristoylphosphatidylcholine; DHPC, dihexanoylphosphatidylcholine; DPPC, dipalmitoylphosphatidylcholine; DOPC, dioleoylphosphatidylcholine; NTA, nitrilotriacetate; TEA, triethanolamine; LUV, large unilamellar vesicle; FID, free induction decay; k_s, scaled rate constant; k_{obs}, observed rate constant; AMBER, assisted model building with energy refinement; TBP, trigonal bipyramidal; MNDO, minor neglect of differential overdays program; QCPE, quantum chemical program exchange.

Correspondence: H.M. Buck, Department of Organic Chemistry, Eindhoven University of Technology, P.O. Box 513, 5600 MB Eindhoven, The Netherlands.

Conductance studies on gramicidin analogues with various peptide residues have indicated that changes in the side-chain conformational flexibility can affect the channel conductance [6]. Furthermore, the importance of the side-chain rotational state on the mean life-time of the channel and hence the transporting properties is also apparent from a previous theoretical study on gramicidin analogues that are not surrounded by other molecules [4,7]. When considering lipid–gramicidin interactions, the conformational distribution of the Trp-15 side-chain is particularly of interest. This residue is situated in the vicinity of the lipid/water interface and, moreover, the molecular structure of the channel entrance might easily be influenced by a change in the rotameric state of this side-chain [4].

In this paper a theoretical and preliminary experimental study is offered on gramicidin–lipid interactions to arrive at a mechanism by which conformational changes can be transferred from the lipid to the polypeptide. It is conceivable that alterations in the gramicidin conformation are brought about by a change in the relative orientation of the lipid carbonyl group and the nearby aromatic Trp-15 side-chain. Support for this idea was gathered by comparing gramicidin properties for the case in which the peptide is surrounded by phospholipids in which the hydrocarbon chains are linked via ester bonds to the glyceryl backbone, as opposed to lipids with ether-linked chains (i.e. without carbonyl groups). Following this approach, information is obtained as to what extent ester lipids can influence the conformation of gramicidin simply by turning away the carbonyl group from the polypeptide. Such reorientation might be the result of conformational changes in the glyceryl backbone of the lipid, which in turn can easily be induced by changes in phospholipid headgroups [2,3].

With AMBER molecular modelling techniques, the gramicidin–lipid interactions were theoretically approached. The gramicidin conformation in the presence of an ether lipid was compared with that in the presence of an ester lipid. It was found that the carbonyl group in acyl lipids can interact via a hydrogen bond with the Trp-15 side-chain of the gramicidin channel, thereby affecting the rotational state of this residue. The importance of this H-bond was underlined by similar calculations on systems consisting of ether or ester lipids and a gramicidin A analogue, in which the tryptophans are substituted by phenylalanines, lacking a hydrogen capable of H-bond formation with the lipids (gramicidin M).

Molecular modelling based on AMBER force-field calculations was originally developed for nucleotides and proteins [9]. Since no data on phospholipids are yet included in the AMBER program, force-field constants for specific lipid groups have to be supplemented to enable the theoretical study of lipid–protein interactions.

To get an indication of the correctness of the molecular modelling study, a preliminary experimental study was carried out by preparing a set of LUVs containing ether and ester lipids. The gramicidin-mediated Na^+ efflux was monitored using ^{23}Na-NMR spectroscopy. The resonances of the external and internal Na^+ ions

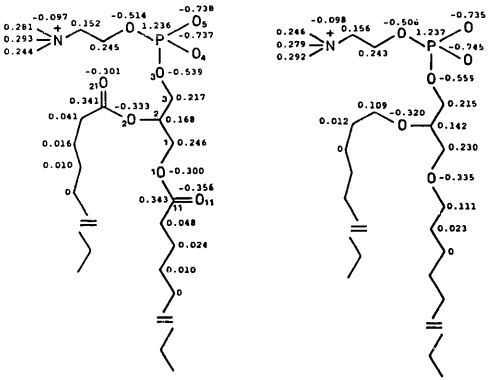

Fig. 1. Atom numbering and charge distribution in DPPC and DHPC derived from calculations based on MNDO.

TABLE I

Relevant torsion angles in DPPC, DHPC, DMPC·2H$_2$O

Notation according to Ref. 14. Torsions in degrees.

	α_1	α_2	α_3	α_4	α_5	α_6	θ_1	θ_2	θ_3	θ_4
DMPC [a]	177	−74	−47	−150	54	176	168	−82	166	51
DPPC [b]	171	−78	−63	−121	66	173	175	−65	177	56
DPPC [c]	167	−76	−67	−123	66	174	171	−68	−175	64
DHPC [d]	179	−71	−69	−122	65	173	171	−67	−168	70
	β_1	β_2	β_3	β_4	β_5	γ_1	γ_2	γ_3	γ_4	γ_5
DMPC [a]	120	179	−134	67	180	102	176	180	180	−170
DPPC [b]	123	170	−155	61	−175	81	−178	−175	175	−179
DPPC [c]	94	−173	−147	61	−170	160	−175	127	−175	177
DHPC [d]	88	−173	−177	65	−172	66	−172	−180	−177	−179

[a] Torsions in the crystal structure of DMPC·2H$_2$O [14].
[b] Torsions in DPPC minimized without gramicidin A.
[c] Torsions in DPPC in the vicinity of gramicidin A.
[d] Torsions in DHPC in the vicinity of gramicidin A.

could be separated by adding a shift reagent (the nitrilotriacetate complex of dysprosium(III); Dy(NTA)$_2^{3-}$) to the vesicle suspension. The change in signal intensity for both kinds of Na^+ ion is directly related to the kinetics of the transmembrane transport [8].

Procedures for molecular modelling

Starting conformations

A monomer of gramicidin A was built with the modelling program CHEM-X [10]. The conformation was set to a left-handed β-helix with 6.3 residues per turn [11–13]. This geometry was experimentally observed in bilayers made up of ester lipids and ether lipids [13]. The atomic charges of the peptide residues were taken from the Brookhaven Protein Database. This structure was minimized with the AMBER program (vide infra). The molecular structure of DPPC was obtained by connecting the choline moiety of D-glycero-1-phosphorylcholine to dimyristoylphosphatic acid. Both structures are available from the Cambridge Crystallographic Database. The hydrocarbon chains were extended with two methylene units each. The torsion angles of the DPPC thus obtained were adjusted according to values in the crystal structure of the dihydrate of DMPC [14]. The electron density in the headgroup and glyceryl backbone was calculated with the QCPE version of MNDO [15] and is depicted in Fig. 1. The ether lipid DHPC was obtained by replacing the carbonyls in the ester moiety by methylene fragments. The relevant torsion angles of the lipids obtained in this way are listed in Table I. Electron densities were again derived from a calculation based on MNDO (Fig. 1). The lipid molecule was positioned near the stacked side-chains of Trp-9 and Trp-15 of the minimized gramicidin with the lipid polar headgroup above the channel opening [16,17]. A forced vertical displacement in both directions of the phospholipid with respect to the gramicidin monomer

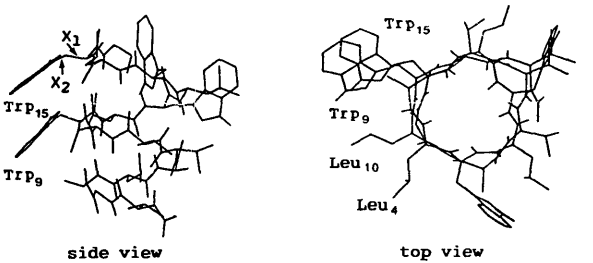

Fig. 2. AMBER-minimized gramicidin structure.

resulted after minimalization in virtually the same conformation as before. Furthermore, we checked the rotational freedom of the Trp-9 and Trp-15 residues around their side-chain torsion angles χ_1 and χ_2 (see Fig. 2 for definitions). The freedom in these angles was approx. 10% with respect to the minimized values without deviating from the well-known β-helix with 6.3 residues per turn [12]. A reoptimalization of a gramicidin geometry with a forced rotation around χ_1 and χ_2 within this range yielded exactly the original minimized conformation.

Gramicidin M was simply obtained by replacing the Trp residues by the Phe side-chains from the Brookhaven Protein Database and minimizing the structure thus obtained.

Computational methods

Energy calculations were performed with the AMBER Molecular Mechanics software package [9], implemented on a VAX 11/780 computer. The empirical energy function is composed of terms that represent bond stretching (I), bending (II), torsions (III), nonbonded Van der Waals and electrostatic interaction terms (IV) as well as hydrogen bond interactions (V):

$$E_{tot} = \underset{\text{bonds}}{\sum} K_r(r - r_{eq})^2 + \underset{\text{angles}}{\sum} K_\theta(\theta - \theta_{eq})^2$$

(I) (II)

$$+ \underset{\text{dihedrals}}{\sum} \frac{V_n}{2}[1 + \cos(n\phi - \gamma)] + \underset{i<j}{\sum}\left(\frac{A_{ij}}{R_{ij}^{12}} - \frac{B_{ij}}{R_{ij}^{6}} + \frac{q_i q_j}{\varepsilon R_{ij}}\right)$$

(III) (IV)

$$+ \underset{\text{H-bonds}}{\sum}\left(\frac{C_{ij}}{R_{ij}^{12}} - \frac{D_{ij}}{R_{ij}^{10}}\right)$$

(V)

Additional force-field parameters for the lipid had to be included in the AMBER parameter set. The values of the lacking constants were based on molecular mechanics calculations on lipids and analogous compounds. In the parameter set thus obtained, small adjustments were made until the AMBER-refined torsion angles of the central DPPC molecule in an assembly of in total seven DPPC lipids, arranged according to a hexagonal lattice, agreed with the crystallographic data on DMPC (Table I) [14]. The optimized, supplemented parameters are compiled in Table II. A distance-dependent dielectric constant, $\varepsilon = R_{ij}$, was used for all calculations, which means that the solvent effect is implicitly taken into account [9,18,19]. The energy is refined by applying a minimization function with analytical gradients until the root mean square of the energy is less than 0.1 kcal/Å. To make the calculation problem manageable for the computer, the united atom model is used. In this model, the hydrogen atoms in CH, CH_2 and CH_3 groups are omitted and their mass and charge are added to the carbon atoms to which they were originally bonded [9].

TABLE II

Supplemented force-field parameters to the AMBER parameter set [a]

Notation according to Ref. 9.

Bond	r_{eq} (Å)	K_r (kcal·mol^{-1}·Å^{-2})
C-HC	1.09 [a]	331.0 [b1]
CH-OS	1.32 [c]	300 [c]
C2-OS	1.32 [c]	400 [c]
C-OS	1.33 [d]	527 [d]
Angle	θ_{eq} (deg)	K_θ (kcal·mol^{-1}·rad^{-2})
HC-C-N	120 [b2]	35.0 [b2]
HC-C-O	120 [b2]	35.0 [b2]
C2-C2-OH	109.5 [b3]	80.0 [b3]
C2-C-OS	109.0 [d]	98 [d]
C-OS-CH	114.0 [d]	64 [d]
C-OS-C2	114.0 [d]	64 [d]
C3-N3-C2	108.0 [d]	90 [d]
OS-C-O	124.0 [d]	190 [d, b4]
C2-OS-CH	111.8 [b4]	100
C3-N3-C3	108.0 [d]	90 [d, b5]
C2-CH-C2	112.4 [b5]	63 [b5]
C3-C2-C2	112.4 [b5]	63
Torsion	$V_n/2$ (kcal/mol)	γ	n
C2-C-OS-CH	3.50 [d]	0 [d]	1 [d]
CH-C-OS-C2	3.50 [d]	0 [d]	1 [d]
C2-C-OS-C2	3.50 [d]	0 [d]	1 [d]
CH-OS-C-O	6.00 [e]	180 [e]	2 [e]
C2-OS-C-O	6.00 [e]	180 [e]	2 [e]
CH-C2-OS-C	1.00 [d]	0 [d]	1 [d]
C2-CH-OS-C	0.35 [d]	0 [d]	1 [d]
OS-C-C2-C2	0.80 [d]	0 [d]	3 [d]

[a] Analogously to values taken from Ref. 41.

[b] Analogously to values taken from Ref. 19: 1. CT-HC; 2. HC-CT-OH HC-C-C HC-CA-C; 3. CH-C2-OH CH-CH-OH C2-CH-OH; 4. C2-OS-C2 C2-OS-C3; 5. CH-C2-C2 CH-C2-C3 C2-C2-C2 CH-C2-CH.

[c] For C-OH, r_{eq} was taken as an average value from the data in Refs. 19 and 42.

[d] Optimized values starting from data in Ref. 44.

[e] Value taken from Ref. 43.

Materials and Methods

Materials

Phospholipids used in these experiments, gramicidin D (containing 80% gramicidin A), Trizma base and the sodium salt of deoxycholic acid were purchased from Sigma. They were used without further purification. Sephadex resins used for gel filtrations were obtained from Pharmacia. All other chemicals used were of analytical reagent grade. $Dy(NTA)_2^-$, the Na^+-shift reagent, was synthesized according to the double heterogeneous reaction [20,21]:

$$Dy_2O_3 + 4H_3NTA + 6TEA \leftrightarrows 6HTEA^+ + 2Dy(NTA)_2^{3-} + 3H_2O$$

To a suspension of 0.75 g Dy_2O_3 and 1.53 g nitrilotriacetate (H_3NTA) in 25 ml water was added dropwise 1.0 ml TEA. In the beginning, the pH should never be allowed to rise above 6–7 to avoid the precipitation of hydroxy salts of dysprosium. Heating the solution up to 70 °C resulted in a clear solution. The pH was 3.5 at that moment. Finally, TEA was added very carefully until a pH of 4.5 was reached. The clear stock solution was diluted 1 : 1 with ^2H_2O and the pH was adjusted to 7 with LiOH, just before addition of the probe to the vesicle suspension.

Methods

LUVs of 100 nm diameter were prepared from a thoroughly dried phospholipid film of typically 18 mg, according to the method described by Enoch and Strittmatter with slight modifications [22]. The lipid film was suspended in a NaCl/Tris-acetate buffer (100 mM NaCl/20 mM Tris-acetate (pH 8.1)) containing 10 mM deoxycholate in a lipid/deoxycholate molar ratio of 2. The suspension was sonicated in a Bransonic 12 ultrasonic bath for 3 min, after which the opaque colour had changed to opalescent. After the formation of LUVs, deoxycholate was removed by passing the sample over two subsequent gel-filtration columns (60 and 30 ml, respectively, of Sephadex G-25M per ml of vesicle suspension; flow rate 100 ml/h) and the collected LUV samples were concentrated to 1 ml by means of an ultrafiltration step (Millipore, Immersible CX-30). In order to prepare a sample for the ^{23}Na-NMR transport studies, external Na^+ was replaced by Li^+ in a third gel-filtration step (20 ml of Sephadex G-50M per ml of vesicle suspension). Care should be taken to avoid any Na^+ contamination at this point, since even small amounts can result in a dramatic decrease in the intravesicular Na^+ fraction (defined as the ratio between the Na^+ amount inside the vesicles and the total Na^+ amount). This would result in a considerably shorter time-interval during which the sodium efflux can be monitored using ^{23}Na-NMR. Elution was performed with 20 mM Tris-acetate buffer (pH 8.1) containing 50 mM LiCl [23] with a flow rate of 10 ml/h. The aqueous solution trapped in the LUVs thus obtained was 100 mM in NaCl, whereas the surrounding aqueous solution was 50 mM in LiCl. After the ion exchange, the collected samples were again concentrated to 1 ml by means of an ultrafiltration step.

Ion efflux measurements

^{23}Na-NMR transport studies were performed according to the method of Pike et al. [8]. After the LUV sample had been transferred to a 10 mm diameter NMR tube, 1 ml of 50 mM LiCl in ^2H_2O was added, as well as 90 μl of a 0.16 M solution of the $Dy(NTA)_2^{3-}$ complex (pH 7.0) as ^{23}Na shift reagent, resulting in a final concentration of 3 mM. In this concentration the shift reagent induces an upfield shift of 0.75 ppm of the external Na^+ signal (Na^+_{out}) with respect to the internal resonance (Na^+_{in}). The ^{23}Na-NMR spectra were recorded on a Bruker CXP-300 NMR spectrometer at 79.4 MHz. 256 FIDs (free induction decays) were accumulated in 102.4 s. The relaxation time of the nuclei was about 0.1 s. The temperature of the measurements was 298 K. By recording five spectra in approx. 30 min, vesicles were checked for leakiness. The ion transport was induced by the addition of 6 μl of a 61.3 mM solution of gramicidin in methanol, resulting in a final concentration in the NMR tube of 0.18 μM in gramicidin. This amounts to approx. eight gramicidin molecules per vesicle (vide infra). Methanol has no influence on the Na^+ transport from vesicles, as was checked in a control experiment in which only methanol was added to a vesicle preparation. After the addition of gramicidin the Na^+ efflux started immediately. This process was followed by recording a series of spectra automatically. A typical kinetics experiment consisted of 20 spectra recorded with 10 s intervals, followed by 10 spectra with 60 s intervals and ultimately 20 spectra with 120 s intervals. The NMR data were plotted as $\ln(R)$ vs. time (t) with R the ratio of fractional area inside at $t = t'$ and the fractional area inside at $t = 0$. The fractional area was defined as the ratio of integrals for Na^+_{in} and Na^+_{out}. The results represent the average of at least two different vesicle preparations.

Determination of the number of gramicidin channels per vesicle

The number of gramicidin channels per vesicle can be calculated from the actual concentration of phospholipids and the number of phospholipid molecules in a 100 nm vesicle [23]. The diameter of the pure DOPC LUVs was checked by inclusion measurements with cytochrome c [24]. It is assumed that 10–20 mol% additions of phospholipids do not alter the mean diameter of the vesicles substantially [25]. Phospholipid concentrations were determined as inorganic phosphate by a modification of the procedure of Bartlet as reported by Litman [26]. The extinction was recorded at 830 nm on a Hitachi 150-20 UV/VIS photospectrometer. Since the phospholipid concentration in the sample varies per vesicle preparation and a fixed quantity of gramicidin is added every time, the number of channels per vesicle is not constant for different preparations. Nonetheless, comparisons can be made when the rate constants are scaled to a fixed number of gramicidin molecules per vesicle (i.e., 12), making use of the quadratic relation between the actual number of gramicidin molecules per vesicle and the observed rate constant [27,28]:

$$k_{obs}/n^2 = k_s/12^2$$

with n, the determined number of gramicidin molecules per vesicle and k_s, the scaled rate constant.

Results

Molecular modelling

The helical torsion angles of the gramicidin backbone ϕ_L, ψ_L and ϕ_D, ψ_D, initially set respectively at $-140°$, $130°$ and $100°$, $-120°$ [12], show after the AMBER energy refinement the presence of a quite large systematical variation with respect to the starting values (Table III). Whereas ϕ_L and ϕ_D decrease from the formyl end towards the channel opening, ψ_L and ψ_D show a steady increase in this direction, starting from D-Val-6. The calculated diameter of the cavity is 3.9 Å and is obtained by subtracting the Van der Waals diameter for the carbonyl oxygen (i.e., 1.6 Å) from the distance between the innermost carbonyl oxygens in the helix core. The calculated length for a monomer is 12 Å. Both features are in close agreement with reported values [16,29]. The AMBER-minimized geometry shows, regarding the stacking of the Trp side-chains 9 and 15, a strong resemblance with other calculated gramicidin structures as well (Fig. 2) [7].

The minimized DPPC-gramicidin A assembly (Fig. 3) shows some interesting features with respect to the lipid–peptide interaction. The indole hydrogen of Trp-15 proves a well-suited interaction site for the phospholipid. Two hydrogen bonds are formed; a strong one with the lipid carbonyl of the *sn*-2 chain with an energy comparable to the intramolecular H-bonds, and a very weak H-bond with the phosphate moiety (Table IV). From the side-chain torsional angles χ_1 and χ_2 (for definitions, see Fig. 2) in Table V, it is concluded that the hydrogen-bond induces a change of 3° in χ_1 and 18° in χ_2 of the Trp-15 side-chain, with respect to the situation with no surrounding molecules. The specific rotation results in a less stacked arrangement of Trp-15 and Trp-9. The conformational distributions in other side-chains are virtually unaffected in the presence of a lipid molecule (data not shown). When DPPC is replaced by the ether lipid DHPC, some pronounced changes

TABLE III

Helical torsion angles of the gramicidin backbone after energy refinement with AMBER

Torsions in degrees, notation according to Ref. 44.

	ϕ			ψ		
	GA	GA/DPPC	GA/DHPC	GA	GA/DPPC	GA/DHPC
L-Val-1	−137	−135	−143	76	76	70
Gly-2	157	150	153	−151	−156	−155
L-Ala-3	−108	−87	−85	85	75	68
D-Leu-4	145	149	149	−139	−135	−139
L-Ala-5	−133	−130	−125	97	107	110
D-Val-6	138	124	120	−176	166	165
L-Val-7	−100	−88	−87	103	102	99
D-Val-8	131	136	136	−146	−133	−125
L-Trp-9	−114	−126	−117	124	120	126
D-Leu-10	107	108	98	−124	−114	−109
L-Trp-11	−132	−140	−142	141	143	141
D-Leu-12	98	95	97	−101	−92	−95
L-Trp-13	−161	−168	−166	152	152	152
D-Leu-14	77	75	73	−96	−89	−88
L-Trp-15	−163	−159	−167	129	129	128

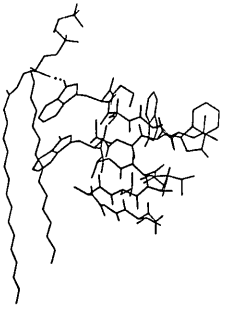

Fig. 3. AMBER-minimized gramicidin A-DPPC assembly. The H-bond between Trp-15 and C=O(21) is denoted by ••.

TABLE IV

Calculated energies of some inter- and intra-molecular H-bonds in the studied gramicidin A-phospholipid assemblies

HNE and HN denote the indole hydrogen of the tryptophan residue and the amide hydrogen, respectively. The nomenclature of the lipid atoms is indicated in Fig. 1. Energies in kcal/mol. These values are only for mutual comparisons and have no absolute meaning.

Origin of bonds	Energy
HNE(Trp-15)-O_{21}(DPPC)	−0.466
HNE(Trp-15)-O_4(DPPC)	−0.002
HNE(Trp-15)-O_4(DHPC)	−0.005
HNE(Trp-15)-O_5(DHPC)	−0.227
HN(Val-8)-O=C(Val-1)	−0.500
HN(Trp-15)-O=C(Trp-13)	−0.122
HN(Trp-15)-O=C(Trp-13) with DPPC	−0.094
HN(Trp-15)-O=C(Trp-13) with DHPC	−0.333

TABLE V

Side-chain torsion angles in gramicidin A after energy refinement

Torsions in degrees.

	χ_1			χ_2		
	GA	GA/DPPC	GA/DHPC	GA	GA/DPPC	GA/DHPC
L-Trp-9	66	71	73	−71	−75	−72
L-Trp-15	68	65	58	−54	−72	−67

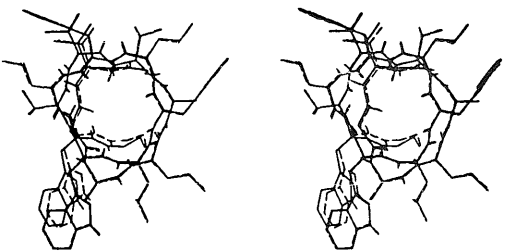

Fig. 4. Stereo view of the AMBER-minimized gramicidin A-DPPC (———) and gramicidin A-DHPC (- - -) assemblies. For clarity, both lipids have been removed.

occur, in particular in the channel entrance area (Fig. 4). The ether lipid interacts with gramicidin A via an H-bond as well, but in this case, a H-bond is formed between Trp-15 and the negatively charged oxygen atoms in the phosphate moiety of DHPC. However, this interaction is weaker than the one between DPPC carbonyl and Trp-15 (Table IV). As a consequence, in the DHPC-gramicidin system the torsion angles χ_1 and χ_2 of the Trp-15 side-chain are changed by approx. 7 and 5°, respectively, with respect to the DPPC-gramicidin assembly (Table V).

An interesting effect of substituting DPPC by DHPC is the small contraction of approx. 0.4 Å of the channel entrance. Such a conformational change in this part of the gramicidin backbone originates from an approx. 10° change in the helix torsion angle ϕ of Trp-9, Trp-15 and Leu-10 (Table III). Furthermore, the contraction seems related to the lowering of the intramolecular H-bond energy between the amide proton of Trp-15 and the carbonyl group of Trp-13 (Table IV).

In order to verify that the lipid-induced conformational changes in the channel entrance are not the result of different dipole–dipole interactions between the lipids and gramicidin, exactly the same procedure was followed for gramicidin M as outlined for the A modification. The phenylalanines in gramicidin M are aromatic, like the tryptophans, but lack a hydrogen capable of forming H-bonds with the lipids. The relative starting positions of the lipids and gramicidin M before AMBER minimization were identical to those in the lipid-gramicidin A assemblies. It appeared that the torsion angles in gramicidin M are virtually unaffected upon the lipid substitution (data not shown). This outcome underlines the conclusion that the H-bond formation in DPPC is essential in affecting the conformational state of gramicidin A.

In order to check whether the conclusions drawn from molecular modelling on gramicidin-lipid systems are subject to the force-field parameter set used, all calculations were also performed with the non-optimized set (vide supra). Despite small variations in the torsion angles of the gramicidin channel and H-bond energies, all conclusions remain valid.

Ion efflux measurements

Fig. 5 shows a typical example of a series of ^{23}Na-NMR spectra, obtained after the addition of gramicidin A to a homogeneous preparation of LUVs with a sodium gradient over the vesicle walls. The vesicles consist of a matrix of DOPC with 10 mol% additions of DPPC or DHPC. This specific composition is chosen to keep the lipid mixture above the phase transition temperature

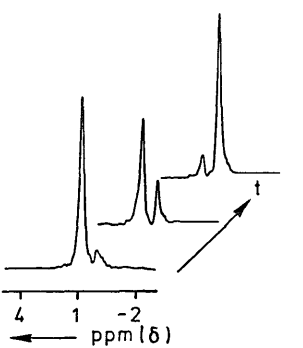

Fig. 5. A series of ^{23}Na-NMR spectra during the time-course of a sodium efflux experiment. The downfield signal originates from Na^+ ions in the vesicles.

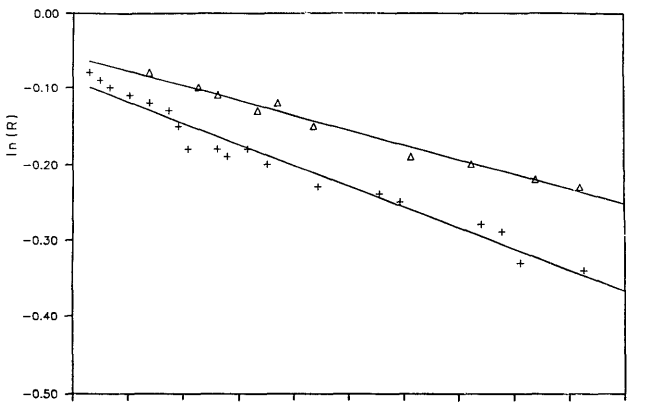

Fig. 6. The evaluated kinetics of an experiment. R is the ratio of integrals for $([Na^+]_{in}/[Na^+]_{out})_{t=t}$ and $([Na^+]_{in}/[Na^+]_{out})_{t=0}$. The kinetics for vesicles with 10 mol% DHPC is denoted by △ and those for 10 mol% DPPC by +.

(approx. 0 °C for 10 mol% DPPC [30]), a prerequisite in the vesicle preparation technique used [22]. Moreover, it is to be expected that vesicle size and fluidity are not much affected on substituting DPPC by DHPC at this concentration [27,31].

It was observed that immediately after the addition of gramicidin to the vesicles, Na^+ efflux is very fast until, after approx. 10 min, a stabilization is reached and the transport decreases exponentially. The cause of the fast transport is unclear at the moment, but it may be related to a disturbance of the lipid bilayer as a consequence of the formation of an ion-conducting gramicidin dimer [32]. When stabilization is reached, the lithium gradient is dissipated by an Na^+–Li^+ exchange, as has been argued previously [8]. After this stage, there is still an Na^+ gradient, which causes Na^+ efflux at the expense of creating a new Li^+ gradient until the diffusion potential of both ions has become equal. However, the latter process starts only after a few hours and is very slow for the vesicles used in this study. Therefore, only the transport rate between approx. 10 and 100 min is considered.

TABLE VI

Scaled Na^+ efflux rate (k_s) through DOPC vesicle walls with 9:1 mol additions of DPPC and DHPC

The actual number of gramicidin channels ranged from three to four per vesicle. (Calculated from the amount of lipids in the sample and the known quantity of added gramicidin, thereby assuming 100 nm vesicles with 85000 phospholipids in a vesicle.) F_{lipid} is the average fraction of initial quantity of lipid found in the vesicles as determined after phosphate analysis. Measurements were carried out at 298 K.

	F_{lipid}	$k_s(\times 10^4)(s^{-1})$
DPPC	0.44	3.7
DHPC	0.49	2.7

See Materials and Methods for definition of efflux rate. The estimated error in the rate constants was less than 10%.

In Fig. 6 the time-course of the Na^+ efflux is plotted for vesicles with DHPC or DPPC. The efflux (R) is given as the ratio of the integrals for the internal and external Na^+ resonances relative to the situation just before the addition of the gramicidin solution. This figure demonstrates that DHPC alters the efflux rate with respect to DPPC. The outcome of this plot is quantified in Table VI from which it can be seen that the Na^+ transport rate decreases by approx. 25% on going from DPPC to DHPC.

Discussion

The AMBER-refined gramicidin A channel (either in the absence or presence of surrounding lipids) reveals in its basic features as pore diameter and channel length a great similarity with the structure computed by Urry et al. [12]. However, the torsion angles of the helical backbone show a considerable, systematic variation along the channel direction. From Fig. 4 and the data in

Table III, in combination with the computed relation between the helical backbone torsion angles and channel diameter [12], it can be concluded that the carbonyls near the channel entrance are turned more inwards to the channel core than those at the formyl end. This result suggests that the ion binding site which is located near the channel opening [16] is already present in the gramicidin molecule and is not formed on the entry of an ion. Indeed, circular dichroism studies have indicated that virtually no changes in the helical pore diameter occur upon ion binding [33].

The most striking result of the present calculations is the formation of a strong hydrogen-bond between the carbonyl group of DPPC and the hydrogen of the indole ring of Trp-15 in the AMBER-minimized gramicidin-lipid assembly. This H-bond brings about a change in the conformational distribution of the Trp-15 size-chain in particular. Such an altered side-chain conformation is accommodated by changes in specific torsion angles in the helical backbone at the entrance of the helix, resulting in a small widening of the channel opening with respect to the conformation in the DHPC-gramicidin assembly. This effect was not found with gramicidin M upon replacing DPPC by DHPC, which strongly indicates that the conformational changes are due to H-bond formation.

The influence of water molecules on the gramicidin conformation should be considered especially in the area of the channel entrance, where, in principle, water molecules might compete with the indole hydrogen in forming an H-bond with the lipid carbonyl oxygen. However, it has been shown using Raman spectroscopy that water molecules do not form H-bonds with the lipid carbonyls [34]. This observation could indicate the absence of water molecules in the direct vicinity of the lipid carbonyl group. Support for this view is found in the crystal structure of diacylglycerol. In this crystal structure, a hydrogen capable of forming H-bonds is properly located with respect to the lipid carbonyl and, as a consequence, a H-bond is observed [25].

The absence of a strong hydrogen-bond with Trp-15 can destabilize the gramicidin dimer conformation in the phospholipid bilayer. Since only the dimer enables the translocation of ions, a decreased lifetime will thus result in a less effective transport. In fact, such an interpretation was previously suggested for the observed decrease in stability of the gramicidin conformation in an ether lipid environment compared with an ester lipid surrounding [36]. Stability was discussed in terms of a specific interaction between the lipid carbonyl and the carboxyl terminus of the channel. Unfortunately, these findings were only very briefly reported, so the precise arguments are unclear. Examination of the gramicidin top-view, however (Fig. 2), reveals that steric interference from the leucine side-groups makes it highly improbable that lipids are situated near the channel-opening and form an H-bond with the hydroxyl group of the carboxyl terminus. Our results indicate a more likely interaction site with gramicidin, based on the vicinity of the lipid carbonyl and the easily accessible hydrogen of Trp-15.

Further, our results on molecular modelling indicate that H-bond formation can lower the energy of the hydrophobic tryptophan residues when directed towards the hydrophilic medium. The presence of an H-bond could very well have been of importance in the semi-empirical conformational analysis of Brasseur et al. [37] on gramicidin A surrounded by lipids. They calculated a slight energetic preference for a gramicidin conformation in which its C-terminus is located in the hydrophobic lipid core relative to the well-known $\beta^{6.3}$ helix in the N–N head-to-head dimer form [11]. To our way of reasoning, their rather surprising outcome might be the result of neglecting the energetic contribution of H-bond formation.

To the best of our knowledge, the theoretically found H-bond has not yet been experimentally observed. Nevertheless, various studies indicate the importance of the indole moiety (with the hydrogen involved) for a proper functioning of the polypeptide. Recently, it was found that on photo-oxidation of the Trp residues, the indole moiety loses the proton and within milliseconds oxidation products are formed. The resulting irreversible loss in conductivity was ascribed to conformational changes near the Trp-containing channel entrance [28,38]. Finally, it was firmly established that a gramicidin analogue in which the hydrogen bonding feature is blocked by the substitution of the indole hydrogens by formyl groups, has lost its ability to induce a non-bilayer arrangement (H_{II} phase) [39,40].

The present findings can be interpreted by proposing a mechanism by which the Na^+ transport can be influenced. The first step in this mechanism is the formation of a five-coordinated TBP phosphorus atom, which changes the conformational equilibrium in the glyceryl backbone of the lipid [2,3]. In the solid phase, this change can lead to an altered chain packing of the lipid hydrocarbon chains (Meulendijks, G.H.W.M., De Haan, J.W., Van Genderen, M.H.P. and Buck, H.M., personal communication), resulting in a shift of the *sn*-2 carbonyl group towards the hydrophobic core. To form an H-bond with maximum energy stabilization, the Trp-15 side-chain orientates to the most basic site available in the lipid. This H-bond is dominated by the orientation of the *sn*-2 lipid-carbonyl group. In order to optimize the H-bond interaction, the Trp-15 side-chain has to adopt a new conformation. Such a change might result in a widening of the channel opening in gramicidin, as is concluded from preliminary calculations in which an assembly with lipids containing five-coordinated TBP phosphorus atoms is compared with lipids containing four-coordinated phosphorus atoms. It could very well

be that the change in the channel entrance area results in an altered ion transport. Hence, the present findings have resulted in a mechanism by which a phospholipid headgroup change can be transmitted via a cascade of conformational changes from the lipid to the protein. Ultimately, this process can result in a change in the efflux rate.

The findings of our theoretical calculations have been checked by a preliminary experimental study in which an increase in Na^+ ion efflux through gramicidin could be observed going from vesicles containing ether lipids to those containing ester lipids. However, a more extensive study of the Na^+ transport rate through gramicidin is needed to get a clear picture of the underlying mechanism of transport.

Concluding remarks

The present molecular modelling study reveals a difference between the two types of lipid in their capacities to form an H-bond with gramicidin. The ester lipid forms a strong H-bond with Trp-15 of the polypeptide, and consequently the channel entrance is larger than in the ether lipid-gramicidin system. The preliminary experiments give a first indication of the influence of the H-bond on the gramicidin-mediated transport through vesicle walls. However, further experiments are necessary to confirm the presence of this specific H-bond interaction between ester lipids and gramicidin. If so, an effective mechanism exists via which conformational changes in the surrounding lipid environment can ultimately be carried over in alterations in the ion efflux rate.

Acknowledgements

Use of the services and facilities of the Dutch CAOS/CAMM Centre, under the Grant Numbers SON-11-20-700 and STW-NCH-44.0703, is gratefully acknowledged. We wish to thank Dr. L.H. Koole and Dr. J.W. de Haan for their critical reading of the manuscript.

References

1 Boulanger, Y., Schreier, S. and Smith, I.C.P. (1981) Biochemistry 20, 6824–6830.
2 Merkelbach, I.I. and Buck, H.M. (1983) Recl. Trav. Chim. Pays-Bas 102, 283–284.
3 Meulendijks, G.H.W.M., Van Es, W., De Haan, J.W. and Buck, H.M. (1986) Eur. J. Biochem. 157, 421–426.
4 Urry, D.W., Venkatachalam, C.M., Prasad, K.U., Bradley, R.J., Parenti-Castelli, G. and Lenaz, G. (1981) Int. J. Quantum Chem. Quantum Biol. Symp. 8, 385–399.
5 Sarges, R. and Witkop, B. (1965) Biochemistry 4, 2491–2494.
6 Heitz, F., Cavach, C., Spach, G. and Trudelle, Y. (1986) Biophys. Chem. 24, 143–148.
7 Urry, D.W. and Venkatachalam, C.M. (1984) J. Comput. Chem. 5, 64–71.
8 Pike, M.M., Sanford, S.R., Balschi, J.A. and Springer, C.S. (1982) Proc. Natl. Acad. Sci. USA 79, 810–814.
9 Weiner, S.J., Kollman, P.A., Case, D.A., Chandra Singh, U., Ghino, C., Alagona, G., Profeta, S. and Weiner, P. (1982) J. Am. Chem. Soc. 106, 765–784.
10 CHEMX/CHEMGRAF, created by Daries, E.K., Chemical Crystallography Laboratory, Oxford University, Developed and distributed by Chemical Design Ltd., Oxford.
11 Urry, D.W., Walker, J.T. and Trapane, T.L. (1982) J. Membr. Biol. 69, 225–231.
12 Venkatachalam, C.M. and Urry, D.W. (1983) J. Comput. Chem. 4, 461–469.
13 Cornell, B.A., Separovic, F., Baldass, A. and Smith, R. (1988) Biophys. J. 53, 67–76.
14 Pearson, R.H. and Pascher, I. (1979) Nature 281, 499–501.
15 Dewar, M.J.S. and Thiel, W. (1977) J. Am. Chem. Soc. 99, 4899–4917.
16 Urry, D.W., Prasad, K.U. and Trapane, T.L. (1982) Proc. Natl. Acad. Sci. USA 79, 390–394.
17 Weinstein, S., Wallace, B.A., Morrow, J.S. and Veatch, W.R. (1980) J. Mol. Biol. 143, 1–19.
18 Moss, R.A., Hendrickson, T.F., Ueoka, R., Kim, K.Y. and Weiner, P.K. (1987) J. Am. Chem. Soc. 109, 4363–4372.
19 Weiner, S.J. and Kollman, P.A. (1986) J. Comput. Chem. 7, 230–252.
20 Merkelbach, I.I., Ph.D. Thesis (1985) Eindhoven University of Technology.
21 Pike, M.M. and Springer, C.S. (1982) J. Magn. Reson. 46, 348–353.
22 Enoch, H.G. and Strittmatter, P. (1979) Proc. Natl. Acad. Sci. USA 76, 145–149.
23 Mimms, L.T., Zamphigi, G., Nozaki, Y., Tanford, C. and Reynolds, J.A. (1981) Biochemistry 20, 833–840.
24 Bangham, A.D., Hill, M.W. and Miller, N.G.A. (1974) Methods Membr. Biol. 1, 1–68.
25 Massari, S. and Colonna, R. (1986) Biochim. Biophys. Acta 863, 264–276.
26 Litman, B.J. (1973) Biochemistry 12, 2545–2554.
27 Hladky, S.B. and Haydon, D.A. (1972) Biochim. Biophys. Acta 274, 294–312.
28 Buster, D.C., Hinton, J.F., Millett, F.S. and Shungu, D.C. (1988) Biophys. J. 53, 145–152.
29 Urry, D.W. (1972) Proc. Natl. Acad. Sci. USA 69, 1610–1614.
30 Furuya, K. and Mitsui, T. (1979) J. Phys. Sco. Japan 46, 611–616.
31 Hauser, H. (1981) Biochim. Biophys. acta 646, 204–210.
32 Clement, N.R. and Gould, J.M. (1981) Biochemistry 20, 1544–1548.
33 Wallace, B.A., Veatch, W.R. and Blout, E.R. (1981) Biochemistry 20, 5754–5760.
34 Bush, S.F., Adams, R.G. and Levin, J.W. (1980) Biochemistry 19, 4429–4436.
35 Pascher, J. and Sundell, S. (1981) J. Mol. Biol. 153, 791–806.
36 Wallace, B.A. (1986) Biophys. J. 49, 295–306.
37 Brasseur, R., Cabiaux, V., Killian, J.A., De Kruyff, B. and Ruysschaert, J.M. (1986) Biochim. Biophys. Acta 855, 317–324.
38 Busath, D.D. and Waldbillig, R.C. (1983) Biochim. Biophys. Acta 736, 28–38.
39 Killian, J.A., Burger, K.N.J. and De Kruyff, B. (1987) Biochim. Biophys. Acta 897, 269–284.
40 Aranda, F.J., Killian, J.A. and De Kruyff, B. (1987) Biochim. Biophys. Acta 901, 217–228.
41 Allinger, N.L. (1977) J. Am. Chem. Soc. 99, 8127–8134.
42 Dorigo, A.E. and Houk, K.N. (1987) J. Am. Chem. Soc. 109, 3698–3708.
43 Teixera-Dias, J.J.C. and Fausto, R.J. (1986) Mol. Structure 144, 199–213.
44 IUPAC-IUB Commission on Biological Nomenclature (1970) J. Mol. Biol. 52, 1–17.